## Potential Target Journals

### Cell Systems Brief Report / Report

- Brief Reports are concise manuscripts with no more than **two** display items (figures and tables) accompanied by ~**1,500 words** of main text.

- Reports may present no more than **four** display items (figures and tables) and ~**2,500 words** of main text.

### Molecular Cell Short Article

The Short Article format is intended for concise, highly provocative, fully validated findings. Short Articles are organized like Research Articles, but they typically report a single main conceptual point. The main text of Short Articles should not exceed **38,000 characters** (including spaces). They may contain up to **4 display items (figures or tables).**

### MSB Reports

The total character count (including spaces) for Reports, excluding the Methods section, tables and Expanded View material, but including title page, abstract, figure legends and references should not exceed 22,000 characters (the exact character count to be stated on the title page). Reports have, in principle, a maximum of 3 Figures.

### Plos Comp. Bio

# Release from NADPH feedback inhibition increases Pentose Phosphate Pathway flux upon oxidative stress in *E. coli*

# Or

# Reserve flux capacity enables rapid oxidative stress response of *E. coli*

Dimitris Christodoulou, Hannes Link, Tobias Fuhrer, Karl Kochanowski, Luca Gerosa, Uwe Sauer

So far, ~3300 words / 21000 characters

## Abstract

To counteract oxidative stress and build-up of reactive oxygen species (ROS), bacteria evolved various defense mechanisms. The primary defense is reduction of ROS through antioxidant systems that must be regenerated through NADPH. To sustain continued ROS reduction, NADPH formation must be increased by increasing flux through replenishing metabolic pathways such as the pentose phosphate (PP) pathway. Here we investigate the mechanism that enables the initial rapid increase in NADPH supply by exposing growing *E. coli* to hydrogen peroxide and quantifying the immediate metabolite dynamics. To systematically infer active regulatory interactions, we developed a framework that allows the evaluation of an ensemble of thousands of kinetic models of glycolysis and PP pathway with different regulation mechanisms. In addition to the known inactivation of the GAP dehydrogenase by ROS, our results signify the important regulatory role of the previously overlooked allosteric inhibition of the first PP pathway enzyme by NADPH. We find that this NADPH feedback inhibition acts as a valve, rapidly increasing the flux through the PP pathway upon oxidative stress. Cells with reduced capacity in rerouting their flux through the PP pathway, show increased sensitivity upon exposure to oxidative stress.

## Introduction

Bacteria like *Escherichia coli* are constantly exposed to environmental challenges, from altering nutrient availability to different types of stresses. Hydrogen peroxide ($H_2O_2$) stress and aerobic metabolism in general, promote the production of reactive oxygen species (ROS) that chemically damage cellular components (Imlay 2013; Mishra & Imlay 2012) and have detrimental effects on metabolism and physiology. To counter such effects, cells have evolved a set of responses that are essential in alleviating the acute cellular damages induced by oxidative stress. Such responses include regulation of metabolic activities in a coordinated fashion, both on short and longer time scales (Baez & Shiloach 2013; Blanchard et al. 2007; Greenberg & Demple 1989; Mishra & Imlay 2012; Rui et al. 2010a; Shimizu 2013; Brumaghim et al. 2003; Grant 2008; Krüger et al. 2011; Ralser et al. 2009).

For *E. coli*, long term defense against ROS is coordinated by the transcription factors OxyR and the SoxRS [REFERENCE OF RECENT REVIEW MISSING], where OxyR responds mostly to $H_2O_2$ stress (Nunoshiba et al. 1992). Since changes in gene expression require at least several minutes to become effective (Chechik et al. 2008), short-responses are based on already present anti-oxidative systems such as superoxide

dismutase, catalases, glutathione peroxidase and non-enzymatic antioxidants like reduced glutathione to scavenge ROS (Finkel 2003; Kohen & Nyska 2002) continuously. To replenish the pool of reduced glutathione, carbon metabolism provides the necessary redox cofactors. Under oxidative stress conditions, it is important for the cell to stabilize its redox state immediately; failing to do so could lead to severe disruption of its biochemical reactions and potentially to its death. Regulation in the short time scale is thus extremely important and indeed *E. coli* and other organisms have in place mechanisms of increasing the conversion rate of $NADP^+$ to NADPH, mainly by rerouting their glycolytic flux into the pentose phosphate (PP) pathway (Ralser et al. 2007a; Rui et al. 2010b; Kuehne et al. 2015; Anastasiou et al. 2011), which under growth on glucose provides approximately 45% of the required NADPH for the cell(Fischer & Sauer 2003)(Fuhrer & Sauer 2009). However, there is surprisingly little understanding on how fast this immediate rerouting of glycolytic flux to PP pathway is, and more importantly which mechanisms matter the most and at which time point in order to implement this metabolic decision.

The current model that describes the rerouting of flux after a few minutes of exposure to oxidative stress, suggests that direct oxidation of lower glycolytic enzymes (e.g. glyceraldehyde 3-phosphate dehydrogenase) creates a blockage in lower glycolysis and leads to accumulation of intermediate glycolytic metabolites and thereby mediates increase in flux through the PP pathway (Ralser et al. 2007b; Ralser et al. 2009). However, the blockage in lower glycolysis alone cannot explain the rerouting of glycolytic flux to PP pathway after a few minutes, as it is thermodynamically challenging to reverse the flux at the pfk - fbpase node (Link et al. 2013a). What is more, if oxidation of the lower glycolytic enzymes was sufficient for the flux rerouting, increased levels of hexoses would have to precede accumulation of PP pathway intermediates, upon oxidative stress. This is not the case in our study, where glycolytic intermediates either do not increase, or increase slower than the PP pathway metabolites (Fig 2A). Recent evidence seem to be in line with our observations and contradict the current model, suggesting that direct regulation of the PP pathway is needed in order to explain the observed metabolite dynamics in mammalian cells (Kuehne et al. 2015).

In the present study, we set out to characterize the immediate metabolic response of *E. coli* to oxidative stress mediated by $H_2O_2$ and answer the question of what matters most and when, in order for flux to be rerouted through PP pathway. We focus on the first seconds (up to one minute) after the exposure of the cells to $H_2O_2$, a time frame that allows us to safely assume that any observed change in metabolite levels or fluxes cannot be caused by transcriptional regulation. We use a combination of short-term dynamic metabolomics measurements and 13C labeling experiments which we integrate in a computational modelling framework, in order to better understand the function of the molecular regulatory mechanisms that allow cells to cope with oxidative stress, in short-time scale. Our results and analyses challenge the current model for flux rerouting through the PP pathway and highlight the important function of allosteric regulation in the cell's response to oxidative stress.

## Results

To identify the time scale of the immediate oxidative stress response, we challenged *E. coli* cultures growing exponentially on glucose with 1mM $H_2O_2$ using a variant of the filter cultivation method (Yuan et al. 2008; Link et al. 2013b), allowing us to sample on a seconds scale. Intracellular changes amongst 50 central metabolites were measured and quantified, occurred already within 5 seconds of $H_2O_2$ exposure (Fig 2A) with the response mostly reflected in the pathways of Glycolysis and PP pathway, with TCA cycle reflecting changes only in few metabolites (Supp. Fig XX).

A closer look at the metabolites in glycolysis reveals that hexose phosphates levels do not increase over time, whereas fructose -1,6 bisphosphate (FBP) levels show a somewhat slow but continuous elevation in the first 30 seconds. Metabolites in lower glycolysis and especially phosphoenolpyruvate (PEP) rapidly decrease after exposure to oxidative stress. Taken together, glycolysis intermediates do not show a consistent trend in their response. The strongest short-term increase was observed for 6-phosphogluconate (6PG), the first metabolite of the oxidative branch of PP pathway. Generally the levels of the PP pathway intermediates show a synchronous, consistent, rapid initial response after 5 seconds of stress, that resembles that of 6PG. This initial overshooting response is attenuated after one minute (Fig 2A). What is more, levels of the redox factor NADPH drop drastically immediately (5 seconds) after the stress (Fig 2A), pointing out to its usage for the scavenging of elevated ROS. Our results are in concordance with data obtained from other organisms (Ralser et al. 2009; Kuehne et al. 2015), that is higher PP pathway metabolites and FBP and decrease in PEP levels, upon exposure to oxidative stress.

The fact that metabolite dynamics change after a few seconds of exposure to stress, especially in the PP pathway, indicates that changes in fluxes also occur at the same time scale. To quantify the actual flux changes after the exposure of cells to $H_2O_2$ mediated stress, we performed stable isotope tracer experiments at the same time scale, switching/perturbing growing batch cultures between 12C glucose and 13C glucose supplemented with $H_2O_2$, using as control a switch between 12C glucose and 13C glucose without $H_2O_2$ supplementation (Supp Fig XX). Quantification of isotopic labeling by mass spectrometry revealed that after 30-60 seconds, cells increase their flux through PP pathway by about 13-20%, as a response to oxidative stress (Fig XX). This result strongly points to the fact that cells do not use *all* the available flux capacity of the oxidative PP pathway enzymes in Glucose mediated growth. (agreeing with recent findings [Davidi COB review, in case it is out soon]). This under-utilization of the oxidative PP pathway enzymes allows cells to increase the flux through these enzymes, if needed. This reconfiguration of flux we observe, already after a few seconds, allows the cell to cope with the depletion of its NADPH pools (Fig2A) and better cope with oxidative stress, as has been also been observed in previous works (Rui et al. 2010b; Kuehne et al. 2015). The time scale of the flux reconfiguration precludes any causal role of transcriptional regulation, but rather requires metabolic regulation mediated either through substrate (e.g. decrease in a specific flux because its reactant decreased) or allosteric regulation.

To explore the mechanistic nature of the observed rapid flux rerouting and obtain a better understanding of the functional role of metabolic regulation, we implemented a kinetic model of glycolysis and PP pathway, linked through $NADP^+$ and NADPH with an abstraction of the glutathione mechanism (Fig 1A). The model includes reversible and irreversible reactions, whose kinetics are

modeled with mass action and Michaelis-Menten laws respectively. The binding constants ($K_m$) were randomly sampled from a range of 0.1-10 times their literature value, in order to account for potential uncertainty, and maximum reaction rates ($V_{max}$) were calculated from flux distributions during steady state growth on glucose, as described before (Link et al. 2013b). The kinetic model consists of 12 ordinary differential equations and can provide predictions for the concentration of 12 metabolites and fluxes of 26 reactions.

We first used the kinetic model framework, to challenge the current model of PP pathway flux rerouting upon stress which suggests that inhibition of the glycolytic enzyme glyceraldehyde 3-phosphate dehydrogenase is enough to explain the metabolite dynamics and flux rerouting (Ralser et al. 2007b; Ralser et al. 2009). To reflect this, we added a direct inhibitory interaction from ROS to lower glycolysis to our computational kinetic model of glycolysis and PP pathway. We performed simulations, varying both the inhibitory effect of ROS and the binding constants of the enzymes that are considered in the model, and compared the results with the experimental metabolite data we generated. Despite the fact that the simulated results can explain to an extent the metabolite dynamics of glycolytic intermediates (SupFig XX), the kinetic model completely fails to describe the metabolite dynamics of the PP pathway metabolites. This result suggests that this inhibitory interaction, although necessary, is not sufficient to explain the metabolite dynamics a few seconds to a minute after exposure to oxidative stress, a conclusion that has also been discussed recently (Kuehne et al. 2015).

If not blockage of lower glycolysis by increasing ROS levels alone is not enough, what more is necessary in order to explain the metabolite dynamics and the PP pathway flux rerouting? We hypothesize that besides the known direct inhibitory effect of ROS on lower glycolysis, additional allosteric regulation must be necessary for the observed rapid flux rerouting upon induction of oxidative stress and proceed to identify these interactions by means of ensemble modelling (Fig 3A) (Kuepfer et al. 2007; Link et al. 2014). Search for the correct regulatory topology of a biochemical network even of this size is a computationally challenging problem (Link et al. 2014). To overcome it, we designed and implemented a scalable computational framework, which allows us to run thousands of simulations in parallel, making it possible to examine hundreds of thousands of topologies and parameter sets fast and efficiently (FigXX). We use this framework to identify allosteric effectors that have a functional role *in vivo*, by augmenting the kinetic model with single, allosteric metabolite-enzyme interactions using a power law term that affects the maximum reaction rates of enzymes (Link et al. 2013a). To avoid a bias through pre-existing knowledge, we consider all combinations of allosteric activation and inhibition for the nine irreversible enzymes by all nine metabolites in the model, yielding 162 potential interactions. The 162 different topologies, each consisting of the core biochemical network with the known effect of ROS on lower glycolysis plus a single allosteric interaction, were then evaluated based on their capacity to explain the experimentally observed metabolite dynamics. For each of the 162 model topologies we sampled the parameter space 10000 times and for each parameter set we simulated the model and compared the model predictions with the experimental data, using the Akaike information criterion (AIC) (Turkheimer et al. 2003), which measures information content and penalizes additional interactions/parameters (SupFig XX).

More than ten interactions improved the model with no allosteric interaction, with the majority of them targeting the first PP pathway enzyme glucose-6-phosphate dehydrogenase (G6PDH), suggesting that

regulation of this enzyme – and the PP pathway in general – is highly important for the response to oxidative stress (SupTable XX). The best model topology though, was the one that included the inhibition of G6PDH by NADPH. This feedback inhibition of the key cofactor NADPH seems crucial (Stincone et al. 2014; Fang et al. 2002)(Sanwal 1970a), as it integrates the information of oxidative stress and seems to be instrumental in the implementation of the rapid metabolic response to stress. NADPH levels drop immediately and G6PDH, which under growth on Glucose is not using all its flux capacity, is now alleviated by its inhibition, allowing more flux through it and thus replenishing NADPH levels which stabilize already after 10 seconds (Fig 2, SupFigXX). We next expanded our modelling approach to include not only single interactions, but this time pairwise interactions, in order to better explore the space of allosteric interactions. Again, the results of our analysis highlight NADPH inhibition of G6PDH as the most prominent interaction, accompanied by the known allosteric activation of the enzyme pyruvate kinase by FBP and also the putative inhibition of G6PDH by FBP (Figure 3C, needs curation). We conclude that the most important allosteric interaction that allows flux to be rerouted immediately to PP pathway is the allosteric inhibition of G6PDH by NADPH. We performed in vitro enzyme assays in order to verify whether NADPH is an inhibitor of G6PDH and characterize its kinetics. Consistent with earlier findings (Sanwal 1970b)(Olavarría et al. 2012), our results clearly show that NADPH is an inhibitor of G6PDH (Sup. Fig XX).

It seems that *E. coli*, under normal growth on Glucose, has some reserve flux capacity in the enzyme G6PDH, and the PP pathway in general, implemented by a combination of NAPDH inhibition and non - saturated G6P concentrations (Supplementary Material). This explains why the previously determined intracellular net fluxes (Fuhrer et al. 2005; Sauer et al. 2004) were about 50% of determined crude cell extract activities of G6PDH. Our hypothesis is that this reserve flux capacity is related with the ability of the cells to cope with oxidative stress: by rerouting the glycolytic flux through PP pathway immediately, cells manage to stabilize their NADPH levels until transcriptional or other regulatory events take over. Cells that lack such plasticity, unable to rapidly increase the flux through PP pathway, should have increased sensitivity when exposed to oxidative stress. To test this hypothesis, we utilized *E. coli* strains that lack the enzyme glucose-6-phosphate isomerase, pgi (Δpgi), and are therefore forced to use PP pathway exclusively when growing on Glucose. In this case, G6PDH is operating – as expected – very close to its apparent $V_{max}$ (Supplementary Material), giving the cells minimal plasticity to rapidly increase the flux through PP pathway. We exposed wild type (WT) and Δpgi *E. coli* strains, exponentially growing in Glucose minimal medium, to oxidative stress in a similar way as we had done for the metabolomics experiments, this time performing multiple parallel experiments with different exposure to $H_2O_2$ mediated stress, ranging from 0.5 mM to 20mM (Materials and Methods, Supplementary Material). This time we focused on the post-stress growth of the cells, in order to evaluate the sensitivity of the two different strains to oxidative stress. Consistent with our hypothesis and earlier findings (Valdivia-González et al. 2012)(Byrne et al. 2014), our thorough analysis reveals that Δpgi *E.coli* strain is more sensitive to $H_2O_2$ mediated stress, evident by the different Minimal Inhibitory Concentration (MIC) levels: 10 mM for Δpgi against 20mM for WT (Supplementary Material).

**Comment: Last minute part, just so you have an idea how this last paragraph will look like:**

Finally, given the important role G6PDH seems to have in oxidative stress response (Sandoval et al. 2011; Zhao et al. 2004; Hua et al. 2003) and the reserve flux capacity we find cells to have in place, we

hypothesized that the sensitivity of *E. coli* to oxidative stress should scale with the reserve flux capacity they have. We engineered a titratable G6PDH (zwf) *E. coli* strain, and asked how the different levels of the enzyme – and therefore different levels of reserve capacity – behave when exposed to different levels of oxidative stress. We hypothesized that the lower the capacity (lower enzyme) the higher the sensitivity of the cells to oxidative stress. Our results confirm our hypothesis and demonstrate that cells with lower enzyme levels (lower reserve capacity) are much more sensitive to oxidative stress when compared to cells with higher enzyme levels (Fig XX). This finding provides strong evidence about the importance of the reserve mechanism cells have in place, which is implemented by NADPH inhibition of G6PDH and seems to play a crucial role in the oxidative stress response.

## Discussion

One of the most difficult questions in systems biology is related to the identification of the functional role of interactions (Gerosa et al. 2015), be it transcriptional, allosteric or post translational. Identifying *in-vivo* functional regulatory interactions is a daunting task, especially in a time scale of seconds, where data at this resolution is not always easy to be obtained and computational analyses are far from trivial. Here, we study the metabolic adaptation of *E. coli* after $H_2O_2$ induced oxidative stress, with an unprecedented time resolution that allowed us to explore the response of the cells after a few seconds of induction. By combining physiology, metabolomics and $C^{13}$ labelling experiments, in vitro derived quantitative kinetic information, biochemical knowledge, mathematical modelling, and genetic perturbations, we were able to discover and identify the functional role of a previously overlooked (in-vitro) allosteric interaction and quantify its effect over time, during the rapid response of *E. coli* to oxidative stress. Through our data and analysis we generated hypotheses regarding the regulatory logic behind the intricate regulatory circuitry and went on to reverse engineer it, and validating our understanding using genetically engineered strains.

We found that cells do not fully utilize the flux capacity of the oxidative PP pathway enzyme G6PDH under growth on Glucose, a decision that is implemented through the allosteric inhibition of the enzyme by the cofactor NADPH. Feedback inhibition of G6PDH by NADPH allows cells to maintain some flux capacity in reserve under normal growth, making them able to rapidly respond to oxidative stress. Thus, this metabolite-enzyme interaction works like a valve in the system: scavenging of the stress-mediated elevated ROS levels depletes NADPH pools, which in turn alleviate the inhibition of G6PDH and allow the enzyme to carry more flux, bringing it closer to its optimal flux capacity. Thereby, cells increase the PP pathway flux by ~20% almost instantaneously and in this way, manage to rebalance their redox state and stabilize the useful NADPH pools. We showed that cells which lack such plasticity and cannot rapidly reroute their flux, like Δpgi mutants, are much more sensitive to oxidative stress. What is more, we showed that cells with lower reserve capacity – we used titratable G6PDH enzyme levels as proxy – are also much more sensitive to $H_2O_2$ induced oxidative stress, highlighting the importance of the mechanism we described.

## References


Anastasiou, D. et al., 2011. Inhibition of pyruvate kinase M2 by reactive oxygen species contributes to cellular antioxidant responses. *Science (New York, N.Y.)*, 334(6060), pp.1278–83. Available at: http://www.pubmedcentral.nih.gov/articlerender.fcgi?artid=3471535&tool=pmcentrez&rendertype=abstract [Accessed April 9, 2015].

Baez, A. & Shiloach, J., 2013. Escherichia coli avoids high dissolved oxygen stress by activation of SoxRS and manganese-superoxide dismutase. *Microbial cell factories*, 12, p.23. Available at: http://www.pubmedcentral.nih.gov/articlerender.fcgi?artid=3605374&tool=pmcentrez&rendertype=abstract [Accessed July 10, 2014].

Blanchard, J.L. et al., 2007. Rapid changes in gene expression dynamics in response to superoxide reveal SoxRS-dependent and independent transcriptional networks. *PloS one*, 2(11), p.e1186. Available at: http://www.pubmedcentral.nih.gov/articlerender.fcgi?artid=2064960&tool=pmcentrez&rendertype=abstract [Accessed June 18, 2014].

Brumaghim, J.L. et al., 2003. Effects of Hydrogen Peroxide upon Nicotinamide Nucleotide Metabolism in Escherichia coli: CHANGES IN ENZYME LEVELS AND NICOTINAMIDE NUCLEOTIDE POOLS AND STUDIES OF THE OXIDATION OF NAD(P)H BY Fe(III). *Journal of Biological Chemistry*, 278(43), pp.42495–42504. Available at: http://www.jbc.org/cgi/doi/10.1074/jbc.M306251200 [Accessed October 11, 2016].

Byrne, R.T. et al., 2014. Escherichia coli genes and pathways involved in surviving extreme exposure to ionizing radiation. *Journal of bacteriology*, 196(20), pp.3534–45. Available at: http://www.ncbi.nlm.nih.gov/pubmed/25049088 [Accessed October 12, 2016].

Chechik, G. et al., 2008. Activity motifs reveal principles of timing in transcriptional control of the yeast metabolic network. *Nature Biotechnology*, 26(11), pp.1251–1259. Available at: http://dx.doi.org/10.1038/nbt.1499 [Accessed April 14, 2015].

Fang, Y.-Z., Yang, S. & Wu, G., 2002. Free radicals, antioxidants, and nutrition. *Nutrition (Burbank, Los Angeles County, Calif.)*, 18(10), pp.872–9. Available at: http://www.ncbi.nlm.nih.gov/pubmed/12361782 [Accessed November 2, 2015].

Finkel, T., 2003. Oxidant signals and oxidative stress. *Current Opinion in Cell Biology*, 15(2), pp.247–254. Available at: http://www.sciencedirect.com/science/article/pii/S0955067403000024 [Accessed June 4, 2015].

Fischer, E. & Sauer, U., 2003. Metabolic flux profiling of Escherichia coli mutants in central carbon metabolism using GC-MS. *European journal of biochemistry*, 270(5), pp.880–91. Available at: http://www.ncbi.nlm.nih.gov/pubmed/12603321 [Accessed December 22, 2016].

Fuhrer, T., Fischer, E. & Sauer, U., 2005. Experimental identification and quantification of glucose metabolism in seven bacterial species. *Journal of bacteriology*, 187(5), pp.1581–90. Available at: http://www.ncbi.nlm.nih.gov/pubmed/15716428 [Accessed December 22, 2016].

Fuhrer, T. & Sauer, U., 2009. Different biochemical mechanisms ensure network-wide balancing of reducing equivalents in microbial metabolism. *Journal of bacteriology*, 191(7), pp.2112–21. Available at: http://www.ncbi.nlm.nih.gov/pubmed/19181802 [Accessed December 22, 2016].

Gerosa, L. et al., 2015. Pseudo-transition Analysis Identifies the Key Regulators of Dynamic Metabolic Adaptations from Steady-State Data. *Cell Systems*, 1(4), pp.270–282. Available at: http://www.cell.com/article/S2405471215001465/fulltext [Accessed October 26, 2015].

Grant, C.M., 2008. Metabolic reconfiguration is a regulated response to oxidative stress. *Journal of biology*, 7(1), p.1. Available at: http://jbiol.com/content/7/1/1 [Accessed July 10, 2014].

Greenberg, J.T. & Demple, B., 1989. A global response induced in Escherichia coli by redox-cycling agents overlaps with that induced by peroxide stress. *Journal of bacteriology*, 171(7), pp.3933–9. Available at: http://www.pubmedcentral.nih.gov/articlerender.fcgi?artid=210145&tool=pmcentrez&rendertype=abstract [Accessed July 11, 2014].

Hua, Q. et al., 2003. Responses of the central metabolism in Escherichia coli to phosphoglucose isomerase and glucose-6-phosphate dehydrogenase knockouts. *Journal of bacteriology*, 185(24), pp.7053–67. Available at: http://www.ncbi.nlm.nih.gov/pubmed/14645264 [Accessed November 14, 2016].

Imlay, J.A., 2013. The molecular mechanisms and physiological consequences of oxidative stress: lessons from a model bacterium. *Nature reviews. Microbiology*, 11(7), pp.443–54. Available at: http://dx.doi.org/10.1038/nrmicro3032 [Accessed May 23, 2014].

Kohen, R. & Nyska, A., 2002. Oxidation of Biological Systems: Oxidative Stress Phenomena, Antioxidants, Redox Reactions, and Methods for Their Quantification. *Toxicologic Pathology*, 30(6), pp.620–650. Available at: http://tpx.sagepub.com/content/30/6/620 [Accessed June 5, 2015].

Krüger, A. et al., 2011. The pentose phosphate pathway is a metabolic redox sensor and regulates transcription during the antioxidant response. *Antioxidants & redox signaling*, 15(2), pp.311–24. Available at: http://www.ncbi.nlm.nih.gov/pubmed/21348809 [Accessed January 22, 2014].

Kuehne, A. et al., 2015. Acute Activation of Oxidative Pentose Phosphate Pathway as First-Line Response to Oxidative Stress in Human Skin Cells. *Molecular cell*. Available at: http://www.cell.com/article/S1097276515004566/fulltext [Accessed July 22, 2015].

Kuepfer, L. et al., 2007. Ensemble modeling for analysis of cell signaling dynamics. *Nature biotechnology*, 25(9), pp.1001–6. Available at: http://dx.doi.org/10.1038/nbt1330 [Accessed November 9, 2014].

Link, H., Christodoulou, D. & Sauer, U., 2014. Advancing metabolic models with kinetic information. *Current Opinion in Biotechnology*, 29, pp.8–14. Available at: http://www.ncbi.nlm.nih.gov/pubmed/24534671 [Accessed February 17, 2014].

Link, H., Kochanowski, K. & Sauer, U., 2013a. Systematic identification of allosteric protein-metabolite interactions that control enzyme activity in vivo. *Nature Biotechnology*, advance on. Available at:

http://dx.doi.org/10.1038/nbt.2489 [Accessed March 4, 2013].

Link, H., Kochanowski, K. & Sauer, U., 2013b. Systematic identification of allosteric protein-metabolite interactions that control enzyme activity in vivo. *Nature biotechnology*, 31(4), pp.357–61. Available at: http://www.nature.com/nbt/journal/v31/n4/full/nbt.2489.html?WT.ec_id=NBT-201304 [Accessed October 22, 2015].

Mishra, S. & Imlay, J., 2012. Why do bacteria use so many enzymes to scavenge hydrogen peroxide? *Archives of biochemistry and biophysics*, 525(2), pp.145–60. Available at: http://www.pubmedcentral.nih.gov/articlerender.fcgi?artid=3413786&tool=pmcentrez&rendertype=abstract [Accessed July 10, 2014].

Nunoshiba, T. et al., 1992. Two-stage control of an oxidative stress regulon: the Escherichia coli SoxR protein triggers redox-inducible expression of the soxS regulatory gene. *Journal of bacteriology*, 174(19), pp.6054–60. Available at: http://www.pubmedcentral.nih.gov/articlerender.fcgi?artid=207670&tool=pmcentrez&rendertype=abstract [Accessed August 5, 2015].

Olavarría, K., Valdés, D. & Cabrera, R., 2012. The cofactor preference of glucose-6-phosphate dehydrogenase from Escherichia coli- modeling the physiological production of reduced cofactors. *FEBS Journal*, 279(13), pp.2296–2309. Available at: http://doi.wiley.com/10.1111/j.1742-4658.2012.08610.x [Accessed July 8, 2016].

Ralser, M. et al., 2007a. Dynamic rerouting of the carbohydrate flux is key to counteracting oxidative stress. *Journal of biology*, 6(4), p.10. Available at: http://www.pubmedcentral.nih.gov/articlerender.fcgi?artid=2373902&tool=pmcentrez&rendertype=abstract [Accessed February 24, 2014].

Ralser, M. et al., 2007b. Dynamic rerouting of the carbohydrate flux is key to counteracting oxidative stress. *Journal of biology*, 6(4), p.10. Available at: http://jbiol.com/content/6/4/10 [Accessed April 30, 2014].

Ralser, M. et al., 2009. Metabolic reconfiguration precedes transcriptional regulation in the antioxidant response. *Nature biotechnology*, 27(7), pp.604–5. Available at: http://dx.doi.org/10.1038/nbt0709-604 [Accessed April 8, 2014].

Rui, B. et al., 2010a. A systematic investigation of Escherichia coli central carbon metabolism in response to superoxide stress. *BMC systems biology*, 4(1), p.122. Available at: http://www.biomedcentral.com/1752-0509/4/122 [Accessed April 8, 2014].

Rui, B. et al., 2010b. A systematic investigation of Escherichia coli central carbon metabolism in response to superoxide stress. *BMC systems biology*, 4, p.122. Available at: http://www.pubmedcentral.nih.gov/articlerender.fcgi?artid=2944137&tool=pmcentrez&rendertype=abstract [Accessed August 6, 2015].

Sandoval, J.M., Arenas, F.A. & Vásquez, C.C., 2011. Glucose-6-phosphate dehydrogenase protects Escherichia coli from tellurite-mediated oxidative stress. *PloS one*, 6(9), p.e25573. Available at:

http://www.plosone.org/article/info%3Adoi%2F10.1371%2Fjournal.pone.0025573#s1 [Accessed May 22, 2014].

Sanwal, B.D., 1970a. Regulatory mechanisms involving nicotinamide adenine nucleotides as allosteric effectors. 3. Control of glucose 6-phosphate dehydrogenase. *The Journal of biological chemistry*, 245(7), pp.1626–31. Available at: http://www.ncbi.nlm.nih.gov/pubmed/4392411 [Accessed November 1, 2015].

Sanwal, B.D., 1970b. Regulatory mechanisms involving nicotinamide adenine nucleotides as allosteric effectors. 3. Control of glucose 6-phosphate dehydrogenase. *The Journal of biological chemistry*, 245(7), pp.1626–31. Available at: http://www.ncbi.nlm.nih.gov/pubmed/4392411 [Accessed July 8, 2016].

Sauer, U. et al., 2004. The soluble and membrane-bound transhydrogenases UdhA and PntAB have divergent functions in NADPH metabolism of Escherichia coli. *The Journal of biological chemistry*, 279(8), pp.6613–9. Available at: http://www.ncbi.nlm.nih.gov/pubmed/14660605 [Accessed December 22, 2016].

Shimizu, K., 2013. Regulation Systems of Bacteria such as Escherichia coli in Response to Nutrient Limitation and Environmental Stresses. *Metabolites*, 4(1), pp.1–35. Available at: http://www.mdpi.com/2218-1989/4/1/1/htm [Accessed April 14, 2014].

Stincone, A. et al., 2014. The return of metabolism: biochemistry and physiology of the pentose phosphate pathway. *Biological reviews of the Cambridge Philosophical Society*. Available at: http://www.ncbi.nlm.nih.gov/pubmed/25243985 [Accessed September 23, 2014].

Turkheimer, F.E., Hinz, R. & Cunningham, V.J., 2003. On the undecidability among kinetic models: from model selection to model averaging. *Journal of cerebral blood flow and metabolism : official journal of the International Society of Cerebral Blood Flow and Metabolism*, 23(4), pp.490–8. Available at: http://www.ncbi.nlm.nih.gov/pubmed/12679726 [Accessed November 1, 2015].

Valdivia-González, M., Pérez-Donoso, J.M. & Vásquez, C.C., 2012. Effect of tellurite-mediated oxidative stress on the Escherichia coli glycolytic pathway. *BioMetals*, 25(2), pp.451–458. Available at: http://link.springer.com/10.1007/s10534-012-9518-x [Accessed October 12, 2016].

Yuan, J., Bennett, B.D. & Rabinowitz, J.D., 2008. Kinetic flux profiling for quantitation of cellular metabolic fluxes. *Nature protocols*, 3(8), pp.1328–40. Available at: http://www.pubmedcentral.nih.gov/articlerender.fcgi?artid=2710581&tool=pmcentrez&rendertype=abstract [Accessed June 7, 2015].

Zhao, J. et al., 2004. Effect of zwf gene knockout on the metabolism of Escherichia coli grown on glucose or acetate. *Metabolic Engineering*, 6(2), pp.164–174.

Anastasiou, D. et al., 2011. Inhibition of pyruvate kinase M2 by reactive oxygen species contributes to cellular antioxidant responses. *Science (New York, N.Y.)*, 334(6060), pp.1278–83. Available at: http://www.pubmedcentral.nih.gov/articlerender.fcgi?artid=3471535&tool=pmcentrez&rendertype=abstract [Accessed April 9, 2015].

Baez, A. & Shiloach, J., 2013. Escherichia coli avoids high dissolved oxygen stress by activation of SoxRS and manganese-superoxide dismutase. *Microbial cell factories*, 12, p.23. Available at: http://www.pubmedcentral.nih.gov/articlerender.fcgi?artid=3605374&tool=pmcentrez&rendertype=abstract [Accessed July 10, 2014].

Blanchard, J.L. et al., 2007. Rapid changes in gene expression dynamics in response to superoxide reveal SoxRS-dependent and independent transcriptional networks. *PloS one*, 2(11), p.e1186. Available at: http://www.pubmedcentral.nih.gov/articlerender.fcgi?artid=2064960&tool=pmcentrez&rendertype=abstract [Accessed June 18, 2014].

Brumaghim, J.L. et al., 2003. Effects of Hydrogen Peroxide upon Nicotinamide Nucleotide Metabolism in Escherichia coli: CHANGES IN ENZYME LEVELS AND NICOTINAMIDE NUCLEOTIDE POOLS AND STUDIES OF THE OXIDATION OF NAD(P)H BY Fe(III). *Journal of Biological Chemistry*, 278(43), pp.42495–42504. Available at: http://www.jbc.org/cgi/doi/10.1074/jbc.M306251200 [Accessed October 11, 2016].

Byrne, R.T. et al., 2014. Escherichia coli genes and pathways involved in surviving extreme exposure to ionizing radiation. *Journal of bacteriology*, 196(20), pp.3534–45. Available at: http://www.ncbi.nlm.nih.gov/pubmed/25049088 [Accessed October 12, 2016].

Chechik, G. et al., 2008. Activity motifs reveal principles of timing in transcriptional control of the yeast metabolic network. *Nature Biotechnology*, 26(11), pp.1251–1259. Available at: http://dx.doi.org/10.1038/nbt.1499 [Accessed April 14, 2015].

Fang, Y.-Z., Yang, S. & Wu, G., 2002. Free radicals, antioxidants, and nutrition. *Nutrition (Burbank, Los Angeles County, Calif.)*, 18(10), pp.872–9. Available at: http://www.ncbi.nlm.nih.gov/pubmed/12361782 [Accessed November 2, 2015].

Finkel, T., 2003. Oxidant signals and oxidative stress. *Current Opinion in Cell Biology*, 15(2), pp.247–254. Available at: http://www.sciencedirect.com/science/article/pii/S0955067403000024 [Accessed June 4, 2015].

Fischer, E. & Sauer, U., 2003. Metabolic flux profiling of Escherichia coli mutants in central carbon metabolism using GC-MS. *European journal of biochemistry*, 270(5), pp.880–91. Available at: http://www.ncbi.nlm.nih.gov/pubmed/12603321 [Accessed December 22, 2016].

Fuhrer, T., Fischer, E. & Sauer, U., 2005. Experimental identification and quantification of glucose metabolism in seven bacterial species. *Journal of bacteriology*, 187(5), pp.1581–90. Available at: http://www.ncbi.nlm.nih.gov/pubmed/15716428 [Accessed December 22, 2016].

Fuhrer, T. & Sauer, U., 2009. Different biochemical mechanisms ensure network-wide balancing of reducing equivalents in microbial metabolism. *Journal of bacteriology*, 191(7), pp.2112–21. Available at: http://www.ncbi.nlm.nih.gov/pubmed/19181802 [Accessed December 22, 2016].

Gerosa, L. et al., 2015. Pseudo-transition Analysis Identifies the Key Regulators of Dynamic Metabolic Adaptations from Steady-State Data. *Cell Systems*, 1(4), pp.270–282. Available at: http://www.cell.com/article/S2405471215001465/fulltext [Accessed October 26, 2015].

Grant, C.M., 2008. Metabolic reconfiguration is a regulated response to oxidative stress. *Journal of biology*, 7(1), p.1. Available at: http://jbiol.com/content/7/1/1 [Accessed July 10, 2014].

Greenberg, J.T. & Demple, B., 1989. A global response induced in Escherichia coli by redox-cycling agents overlaps with that induced by peroxide stress. *Journal of bacteriology*, 171(7), pp.3933–9. Available at: http://www.pubmedcentral.nih.gov/articlerender.fcgi?artid=210145&tool=pmcentrez&rendertype=abstract [Accessed July 11, 2014].

Hua, Q. et al., 2003. Responses of the central metabolism in Escherichia coli to phosphoglucose isomerase and glucose-6-phosphate dehydrogenase knockouts. *Journal of bacteriology*, 185(24), pp.7053–67. Available at: http://www.ncbi.nlm.nih.gov/pubmed/14645264 [Accessed November 14, 2016].

Imlay, J.A., 2013. The molecular mechanisms and physiological consequences of oxidative stress: lessons from a model bacterium. *Nature reviews. Microbiology*, 11(7), pp.443–54. Available at: http://dx.doi.org/10.1038/nrmicro3032 [Accessed May 23, 2014].

Kohen, R. & Nyska, A., 2002. Oxidation of Biological Systems: Oxidative Stress Phenomena, Antioxidants, Redox Reactions, and Methods for Their Quantification. *Toxicologic Pathology*, 30(6), pp.620–650. Available at: http://tpx.sagepub.com/content/30/6/620 [Accessed June 5, 2015].

Krüger, A. et al., 2011. The pentose phosphate pathway is a metabolic redox sensor and regulates transcription during the antioxidant response. *Antioxidants & redox signaling*, 15(2), pp.311–24. Available at: http://www.ncbi.nlm.nih.gov/pubmed/21348809 [Accessed January 22, 2014].

Kuehne, A. et al., 2015. Acute Activation of Oxidative Pentose Phosphate Pathway as First-Line Response to Oxidative Stress in Human Skin Cells. *Molecular cell*. Available at: http://www.cell.com/article/S1097276515004566/fulltext [Accessed July 22, 2015].

Kuepfer, L. et al., 2007. Ensemble modeling for analysis of cell signaling dynamics. *Nature biotechnology*, 25(9), pp.1001–6. Available at: http://dx.doi.org/10.1038/nbt1330 [Accessed November 9, 2014].

Link, H., Christodoulou, D. & Sauer, U., 2014. Advancing metabolic models with kinetic information. *Current Opinion in Biotechnology*, 29, pp.8–14. Available at: http://www.ncbi.nlm.nih.gov/pubmed/24534671 [Accessed February 17, 2014].

Link, H., Kochanowski, K. & Sauer, U., 2013a. Systematic identification of allosteric protein-metabolite interactions that control enzyme activity in vivo. *Nature Biotechnology*, advance on. Available at: http://dx.doi.org/10.1038/nbt.2489 [Accessed March 4, 2013].

Link, H., Kochanowski, K. & Sauer, U., 2013b. Systematic identification of allosteric protein-metabolite interactions that control enzyme activity in vivo. *Nature biotechnology*, 31(4), pp.357–61. Available at: http://www.nature.com/nbt/journal/v31/n4/full/nbt.2489.html?WT.ec_id=NBT-201304 [Accessed October 22, 2015].

Mishra, S. & Imlay, J., 2012. Why do bacteria use so many enzymes to scavenge hydrogen peroxide?

*Archives of biochemistry and biophysics*, 525(2), pp.145–60. Available at: http://www.pubmedcentral.nih.gov/articlerender.fcgi?artid=3413786&tool=pmcentrez&rendertype=abstract [Accessed July 10, 2014].

Nunoshiba, T. et al., 1992. Two-stage control of an oxidative stress regulon: the Escherichia coli SoxR protein triggers redox-inducible expression of the soxS regulatory gene. *Journal of bacteriology*, 174(19), pp.6054–60. Available at: http://www.pubmedcentral.nih.gov/articlerender.fcgi?artid=207670&tool=pmcentrez&rendertype=abstract [Accessed August 5, 2015].

Olavarría, K., Valdés, D. & Cabrera, R., 2012. The cofactor preference of glucose-6-phosphate dehydrogenase from Escherichia coli- modeling the physiological production of reduced cofactors. *FEBS Journal*, 279(13), pp.2296–2309. Available at: http://doi.wiley.com/10.1111/j.1742-4658.2012.08610.x [Accessed July 8, 2016].

Ralser, M. et al., 2007a. Dynamic rerouting of the carbohydrate flux is key to counteracting oxidative stress. *Journal of biology*, 6(4), p.10. Available at: http://www.pubmedcentral.nih.gov/articlerender.fcgi?artid=2373902&tool=pmcentrez&rendertype=abstract [Accessed February 24, 2014].

Ralser, M. et al., 2007b. Dynamic rerouting of the carbohydrate flux is key to counteracting oxidative stress. *Journal of biology*, 6(4), p.10. Available at: http://jbiol.com/content/6/4/10 [Accessed April 30, 2014].

Ralser, M. et al., 2009. Metabolic reconfiguration precedes transcriptional regulation in the antioxidant response. *Nature biotechnology*, 27(7), pp.604–5. Available at: http://dx.doi.org/10.1038/nbt0709-604 [Accessed April 8, 2014].

Rui, B. et al., 2010a. A systematic investigation of Escherichia coli central carbon metabolism in response to superoxide stress. *BMC systems biology*, 4(1), p.122. Available at: http://www.biomedcentral.com/1752-0509/4/122 [Accessed April 8, 2014].

Rui, B. et al., 2010b. A systematic investigation of Escherichia coli central carbon metabolism in response to superoxide stress. *BMC systems biology*, 4, p.122. Available at: http://www.pubmedcentral.nih.gov/articlerender.fcgi?artid=2944137&tool=pmcentrez&rendertype=abstract [Accessed August 6, 2015].

Sandoval, J.M., Arenas, F.A. & Vásquez, C.C., 2011. Glucose-6-phosphate dehydrogenase protects Escherichia coli from tellurite-mediated oxidative stress. *PloS one*, 6(9), p.e25573. Available at: http://www.plosone.org/article/info%3Adoi%2F10.1371%2Fjournal.pone.0025573#s1 [Accessed May 22, 2014].

Sanwal, B.D., 1970a. Regulatory mechanisms involving nicotinamide adenine nucleotides as allosteric effectors. 3. Control of glucose 6-phosphate dehydrogenase. *The Journal of biological chemistry*, 245(7), pp.1626–31. Available at: http://www.ncbi.nlm.nih.gov/pubmed/4392411 [Accessed November 1, 2015].

Sanwal, B.D., 1970b. Regulatory mechanisms involving nicotinamide adenine nucleotides as allosteric effectors. 3. Control of glucose 6-phosphate dehydrogenase. *The Journal of biological chemistry*, 245(7), pp.1626–31. Available at: http://www.ncbi.nlm.nih.gov/pubmed/4392411 [Accessed July 8, 2016].

Sauer, U. et al., 2004. The soluble and membrane-bound transhydrogenases UdhA and PntAB have divergent functions in NADPH metabolism of Escherichia coli. *The Journal of biological chemistry*, 279(8), pp.6613–9. Available at: http://www.ncbi.nlm.nih.gov/pubmed/14660605 [Accessed December 22, 2016].

Shimizu, K., 2013. Regulation Systems of Bacteria such as Escherichia coli in Response to Nutrient Limitation and Environmental Stresses. *Metabolites*, 4(1), pp.1–35. Available at: http://www.mdpi.com/2218-1989/4/1/1/htm [Accessed April 14, 2014].

Stincone, A. et al., 2014. The return of metabolism: biochemistry and physiology of the pentose phosphate pathway. *Biological reviews of the Cambridge Philosophical Society*. Available at: http://www.ncbi.nlm.nih.gov/pubmed/25243985 [Accessed September 23, 2014].

Turkheimer, F.E., Hinz, R. & Cunningham, V.J., 2003. On the undecidability among kinetic models: from model selection to model averaging. *Journal of cerebral blood flow and metabolism : official journal of the International Society of Cerebral Blood Flow and Metabolism*, 23(4), pp.490–8. Available at: http://www.ncbi.nlm.nih.gov/pubmed/12679726 [Accessed November 1, 2015].

Valdivia-González, M., Pérez-Donoso, J.M. & Vásquez, C.C., 2012. Effect of tellurite-mediated oxidative stress on the Escherichia coli glycolytic pathway. *BioMetals*, 25(2), pp.451–458. Available at: http://link.springer.com/10.1007/s10534-012-9518-x [Accessed October 12, 2016].

Yuan, J., Bennett, B.D. & Rabinowitz, J.D., 2008. Kinetic flux profiling for quantitation of cellular metabolic fluxes. *Nature protocols*, 3(8), pp.1328–40. Available at: http://www.pubmedcentral.nih.gov/articlerender.fcgi?artid=2710581&tool=pmcentrez&rendertype=abstract [Accessed June 7, 2015].

Zhao, J. et al., 2004. Effect of zwf gene knockout on the metabolism of Escherichia coli grown on glucose or acetate. *Metabolic Engineering*, 6(2), pp.164–174.

Figures draft outline:

1) Experimental approach and system on focus
2) Data - results
3) Modelling approach and results

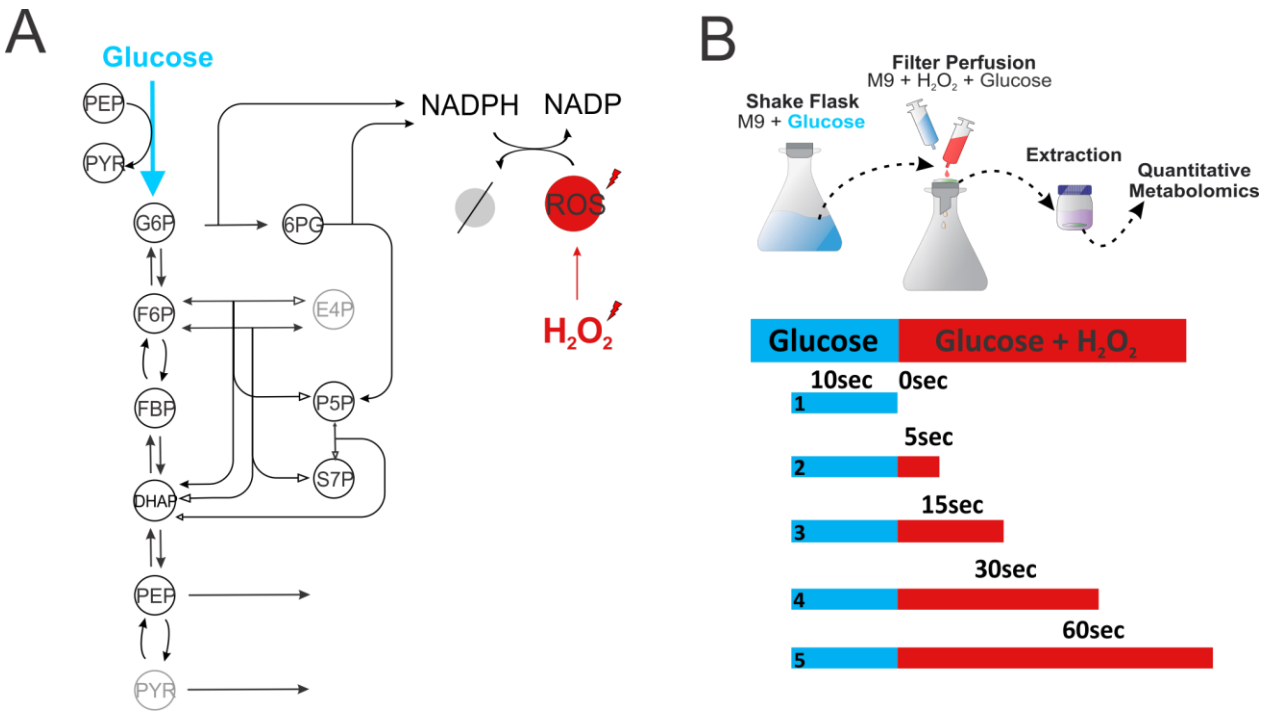


Figure 1

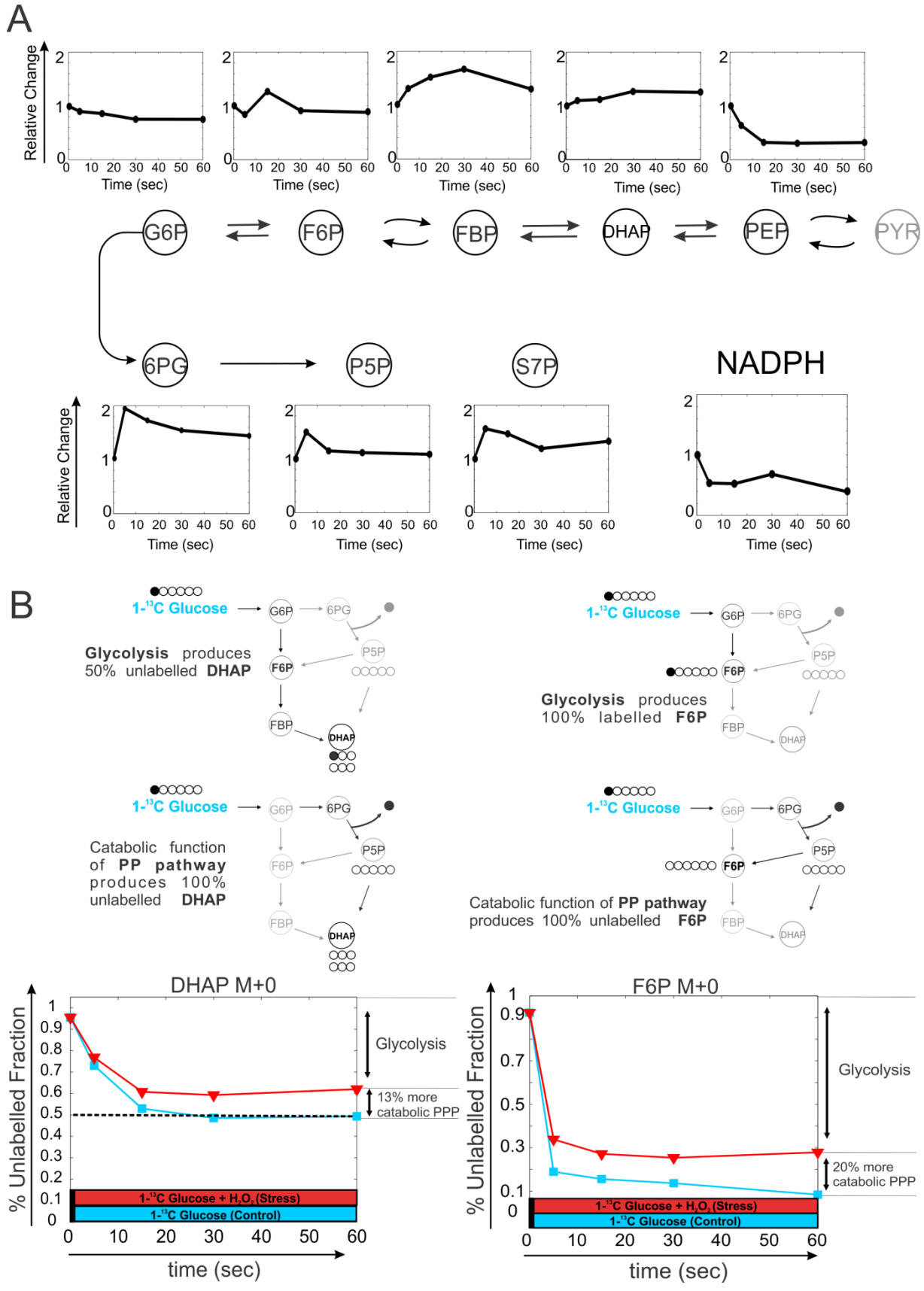
A
Relative Change
Time (sec)
G6P
F6P
FBP
DHAP
PEP
PYR
6PG
P5P
S7P
NADPH
B
1-13C Glucose
Glycolysis produces 50% unlabelled DHAP
Glycolysis produces 100% labelled F6P
Catabolic function of PP pathway produces 100% unlabelled DHAP
Catabolic function of PP pathway produces 100% unlabelled F6P
DHAP M+0
F6P M+0
% Unlabelled Fraction
time (sec)
Glycolysis
13% more catabolic PPP
20% more catabolic PPP
1-13C Glucose + H2O2 (Stress)
1-13C Glucose (Control)

Figure 2

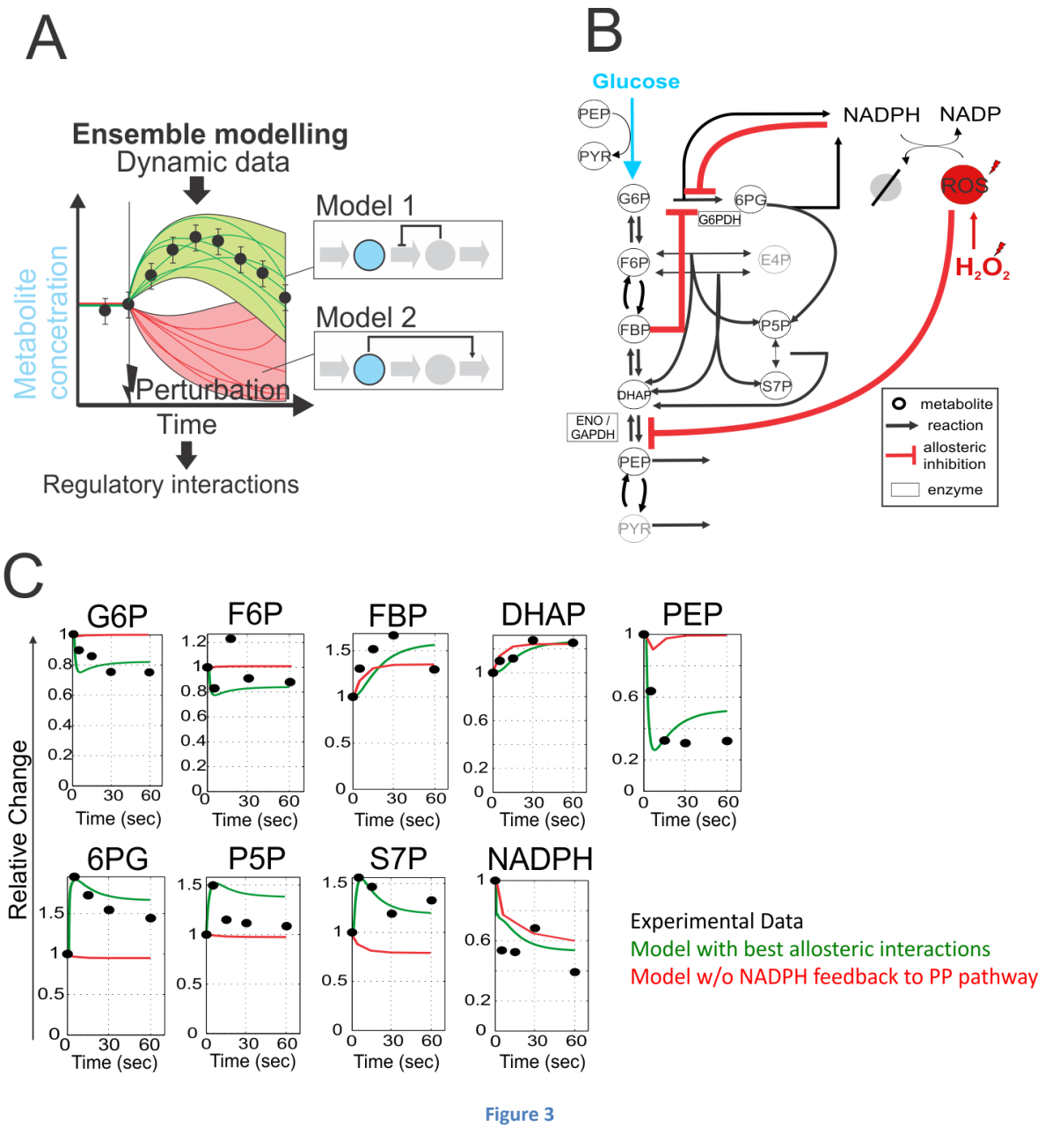
A
Ensemble modelling
Dynamic data
Model 1
Model 2
Metabolite concetration
Perturbation
Time
Regulatory interactions
B
Glucose
PEP
PYR
G6P
6PG
G6PDH
NADPH
NADP
ROS
$H_2O_2$
F6P
E4P
FBP
P5P
DHAP
S7P
ENO / GAPDH
PEP
PYR
metabolite
reaction
allosteric inhibition
enzyme
C
Relative Change
G6P
F6P
FBP
DHAP
PEP
6PG
P5P
S7P
NADPH
Time (sec)
Experimental Data
Model with best allosteric interactions
Model w/o NADPH feedback to PP pathway

Figure 3

## Supplementary Material

In vitro studies ----- Toby

Results

$K_m$ values were from measurements were glucose-6-phosphate concentrations were varied from 50 µM to 400 µM, while the NADP+ concentrations were between 20 µM and 150 µM. The resulting $K_m$ values for NADP+ and glucose-6-phsophate are listed in Table 1. $K_i$ values of NADPH were determined with one substrate kept at a constant concentration, while the second substrate was varied at different constant inhibitor concentrations. According to the determined sequential ordered bi-bi-mechanism it was expected that NADPH will inhibit competitively in respect to NADP+ and mixed non-competitive with respect to glucose-6-phosphate [1]. To determine the respective inhibition constants, reaction velocities were determined under different NADPH concentrations (150, 75 and 0 µM), the glucose-6-phosphate concentration was held at 400 µM and $NADP^+$ was varied from 10 to 60 µM or alternatively $NADP^+$ was held at 40 µM and glucose-6-phosphate was varied from 50 to 400 µM. The resulting inhibition constants and intracellular concentrations are indicated in Table 1.

Table 1 Experimentally determined kinectic parameters and intracellular metabolit concentrations

| | Own data [µM] | Olavarria et al [5] [µM] |
|---|---|---|
| ***Substrate $K_m$*:** | | |
| $NADP^+$ | 23 | 7.5 ± 0.8 |
| glucose-6-phosphate | 136 | 174 ± 11 |
| ***$NADP^+$ dissociation $K_i$*:** | | |
| $NADP^+$ | 90 | 19 ± 4 |
| ***NADPH inhibition $K_i$*:** | | |
| $K_{ic,NADP+}$ | 35 | 14 ± 2 |
| $K_{ic,glucose\text{-}6\text{-}phosphate}$ | 100 | 101 ± 9 |
| ***Intracellular Concentrations*** | | |
| **wild-type** | | |
| Glucose-6-phosphate | 289 ± 2 | 801 |
| $NADP^+$ | 581 ± 13 | 21-210 |
| NADPH | 191 ± 20 | 24-220 |
| ***Δpgi*** | | |
| Glucose-6-phosphate | 3301 ± 41 | - |

| | | |
|---|---|---|
| $NADP^+$ | 400 ± 31 | - |
| NADPH | 211 ± 9x | - |

For the initial rate predictions using intracellular metabolite concentrations shown in Figure 2, the rate laws (equations 1 & 2) describing the forward reaction in the presence of both educts and products were used that were previously published for glucose-6P dehydrogenase in *E. coli* (1). Only the forward reaction with NADPH inhibition was simulated since the 6P-gluconolactone produced reacts rapidly further to 6P-gluconate and in addition is very instable [2].

Methods

*Quantification of intracellular metabolite concentrations*

All measurements were carried out on an Agilent 1100 Series HPLC system coupled with an Applied Biosystems / MDS SCIEX 4000 Q TRAP™. Data were recorded and analyzed with Analyst Software Version 1.4.2 Build 1228. Chromatographic separation was achieved on a Phenomenex Hydro RP 150 mm x 2.1 mm x 4 µm column at 40°C using an adapted version of a published protocol [3]. Briefly, the injected volume was 8 µl, and the mobile phase at a flow rate of 200 µl/min was directly introduced into the mass spectrometer via electro spray ionization (ESI). The gradient profile was linear with two phases (Table 1), where solution A was 10 mM tributylamine and 15 mM acetate in H2O (pH 4.95) and solution B was 100 % methanol. Multiple reaction monitoring (MRM) settings were optimized individually for each metabolite except 6P-gluconolactone for which the MRM settings were adapted from 6P-gluconate [3].

**Table 1** - Gradient profile applied for the LC-MS/MS method

| Step | Total time (min) | Eluent A (vol.%) | Eluent B (vol.%) |
|---|---|---|---|
| 1 | 0 | 100 | 0 |
| 2 | 15 | 45 | 55 |
| 3 | 27 | 34 | 66 |
| 4 | 28 | 0 | 100 |
| 5 | 33 | 0 | 100 |
| 6 | 35 | 100 | 0 |
| 7 | 55 | 100 | 0 |

*Characterization of Glucose-6-phosphate dehydrogenase*

Glucose-6-phosphate dehydrogenase was overexpressed in 50 ml LB medium with 0.1 mM IPTG and 25 mg/L chloramphenicol at 37°C and 250 rpm from an overexpression plasmid obtained from the ASKA clone collection [4]. Cells were harvested by centrifugation and the pellet was washed twice with 2 ml 0.9% NaCl with 10 mM $MgSO_4$. The pellet was then resuspended in 4 ml ice cold 100 mM Tris-HCl pH 7.5, 5 mM $MgCl_2$ supplemented with Protease-Inhibitor (Complete EDTA-free, Roche) and 1 mM DTT. Cells were disrupted by passage through a precooled French press mini cell at 1000 PSI and the crude extract was subsequently centrifuged for 30 min at 23000 x g and 4°C to obtain a clear cell lysate. The lysate was then loaded on a 1ml HisTrap HP columns from Amersham Biosciences. The column was washed with 12 volumes of wash buffer (20 mM NaH2PO4 pH 7.5, 500 mM NaCl, 10 mM Imidazole, 15 mM β-Mercaptoethanol) and then the protein was eluted using increasing imidazole concentrations. Fractions containing pure protein were buffer-exchanged against 100 mM Tris-HCl pH 7.5, 10 mM MgCl2 and 15 mM β-Mercaptoethanol using 25 kD Spectra-Por Float-A-Lyzer.

All enzyme assays were run at 30°C in 100 mM Tris HCl pH7.5 and 10 mM $MgCl_2$ on a Spectramax Plus spectrometer (Molecular Devices). Absorbance was recorded at 340 nm with 2 second interval single measurements in 1 ml cuvettes. Purified enzyme was equilibrate with cofactor until absorbance at 340 nm was stable. The measured absorbance curve over time was regressed with a second order polynomial to determine the initial velocity at the time point when the second substrate was added and the sample was mixed. The $K_m$ values for $NADP^+$ and glucose-6P and the $K_i$ value for NADPH were then obtained by varying respective substrate or inhibitor concentrations and analysis by primary and secondary Lineweaver-Burk plots assuming a sequential two-substrate mechanism [1]:

$$V_{G6PDH} = \frac{V_{\max}\left[NADP^+\right]\left[G6P\right]}{K_{D,NADP^+}K_{m,G6P} + K_{m,G6P}\left[NADP^+\right] + K_{m,NADP^+}\left[G6P\right] + \left[NADP^+\right]\left[G6P\right]} \quad (1)$$

Inhibition by NADPH was determined to be competitive with respect to $NADP^+$ which can be included by the following inhibitory terms (1):

$$V_{G6PDH} = \frac{V_{\max}\left[NADP^+\right]\left[G6P\right]}{K_{D,NADP^+}K_{m,G6P}\left(1+\frac{\left[NADPH\right]}{K_{i,NADPH}}\right) + K_{m,G6P}\left[NADP^+\right] + K_{m,NADP^+}\left[G6P\right]\left(1+\frac{\left[NADPH\right]}{K_{i,NADPH}}\right) + \left[NADP^+\right]\left[G6P\right]} \quad (2)$$

Supplemental Figures

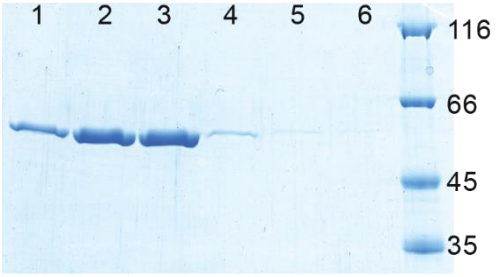


**Suppl. Figure 1** SDS-PAGE of overexpressed and His-Tag purified glucose-6P dehydrogenase (~56.8 kD including His-Tag). The pure enzyme was eluted with different imidazole concentrations (lanes 1 to 6: 100-200, 200, 200-300, 300, and twice 500 mM imidazole). Fractions in lane 2 and 3 were pooled for further analysis.

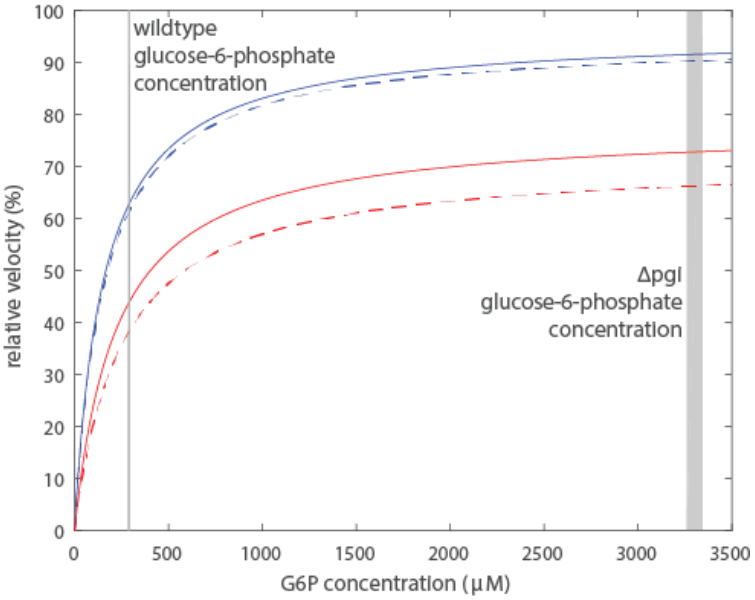


**Suppl. Figure 2** Simulated initial reaction velocities for glucose-6-phosphate dehydrogenase using rate laws without NADPH inhibition (Equation 1) and with NADPH inhibition (Equation 2). Experimentally determined kinetic parameters and intracellular cofactor concentrations were used (Table 1). Intracellular concentrations from wildtype and from pgi knockout are shown with solid and dashed lines respectively. Actual intracellular glucose-6-phosphate concentrations for wildtype and *pgi* knockout are indicated by the grey bars.

**References**


1) Chassagnole, C., et al., *Dynamic modeling of the central carbon metabolism of Escherichia coli.* Biotechnology and Bioengineering, 2002. **79**(1): p. 53-73.
2) Bauer, H. P., T. Srihari, J. C. Jochims, and H. W. Hofer. 1983. 6-phosphogluconolactonase. Purification, properties and activities in various tissues. Eur. J. Biochem. 133:163-168.
3) Luo, B., K. Groenke, R. Takors, C. Wandrey, and M. Oldiges. 2007. Simultaneous determination of multiple intracellular metabolites in glycolysis, pentose phosphate pathway and tricarboxylic acid cycle by liquid chromatography-mass spectrometry. J. Chromatogr. A 1147:153-164.
4) Kitagawa, M., T. Ara, M. Arifuzzaman, T. Ioka-Nakamichi, E. Inamoto, H. Toyonaga, and H. Mori. 2005. Complete set of ORF clones of Escherichia coli ASKA library (a complete set of Escherichia coli K-12 ORF archive): unique resources for biological research. DNA Res. 12:291-299.
5) Karel Olavarrı´a, Diego Valde´ s and Ricardo Cabrera, The cofactor preference of glucose-6-phosphate dehydrogenase from Escherichia coli – modeling the physiological production of reduced cofactors. FEBS Journal 279 (2012) 2296–2309

**Methods section on zwf titration strain**

*Strain construction*

The *zwf* titration strain was constructed as follows. First, the *zwf* gene was cloned into the IPTG-titratable expression plasmid pTrc99KK (Link *et al*, 2013) (primer 1: GCCTCGAGATGGCGGTAACGCAAACAGCC, primer 2: CGGGATCCTTACTCAAACTCATTCCAGGAACG), yielding plasmid pTrc99KK-*zwf*. This plasmid was then transformed into a *zwf* deletion strain obtained from the Keio collection (Baba *et al*, 2006). To exclude adverse effects on oxidative stress resistance merely due to protein overexpression, the *zwf* deletion strain was also transformed with a N-terminal his-tagged GFP titration plasmid, pTrc99KK-GFP:N-term HT, which was obtained from (Nikolaev *et al*, 2016).